MHD Effects on Composite Slider Bearing Lubricated with Couple-stress Fluids

Biradar Kasinath[1] and B. N. Hanumagowda[2]

1. *Department of Mathematics, Government College, Gulbarga -585 105, India.*
2. *Department of Mathematics, East Point College of Engineering & Technology, Bangalore - 560049, India.*

Abstract

A magneto-hydrodynamic wide composite slider bearing lubricated with couple-stress fluids is numerically analysed. A modified Reynolds equation has been derived to account for the transverse magnetic field in the couple-stress fluid lubrication of wide composite slider bearings. The closed form expressions are obtained for the non-dimensional fluid film pressure, load carrying capacity, frictional force and coefficient of friction. It is found that the fluid film pressure, load carrying capacity, frictional force and coefficient of friction increases as the strength of the magnetic field increases. The results are compared with non-magnetic case.

Keywords: Composite slider bearing, Magnetohydrodynamic, Couplestress.

1. Introduction

Slider bearings are designed for supporting the transverse load in engineering systems. The effect of the couple stress on the Slider bearings was studied by Ramanaiah and Sarker [1]. It is shown that the load-carrying capacity and Frictional force are found to increase but the coefficient of friction decrease as compared to the corresponding Newtonian case. Lin et al. [2] analysed the effect of couple stress on plane inclined slider bearings. It is shown that the effect of couple stress is to increase the steady-state and the dynamic stiffness and damping characteristics. Bujurke et al. [3] studied the effect of couple stress on porous slider bearing and shown that the load carrying capacity increases and coefficient of friction decreases for the

increasing values of couple stress parameter. Several investigators [4-10] have studied the lubrication problems with Stokes [11] couple stress fluid as lubricant.

As most MHD bearing models have been developed from the view point of simplicity of mathematical analysis rather than their practicability hence the study of MHD lubrication is much more involved than that of hydrodynamic lubrication. Shukla [12] studied the effect of MHD on composite slider bearing and shown that the load carrying capacity increases as the applied magnetic field increases. Also it is shown that, the load carrying capacity is greater in the case of composite bearing than that of plain slider bearings. MHD steady and dynamic characteristics of wide tapered-land slider bearings was analysed by Lin [13]. It is shown that the effect of magnetic field increases the load carrying capacity and dynamic co efficient as well as decreases the steady friction parameter. Recently, Naduvinamani et al., [14] analysed the effect of MHD on circular stepped bearings lubricated with couple stress fluids. It is shown that the effect of magnetic field increases the load carrying capacity and also lengthens squeeze film time. Several investigators [15-29] studied the lubrication problems with MHD.

The effect of applied transverse magnetic field on the performance of composite slider bearings lubricated with couple-stress fluid has not been studied so far. Hence in this paper the effects of transverse magnetic field on a wide composite slider bearing with couple-stress fluid is analyzed.

2. Mathematical formulation

The magneto-hydrodynamic wide composite slider bearing with couple-stress fluids with a transverse magnetic field is shown in figure 1. The basic equations governing the hydro-magnetic flow of the couple-stress lubricant are

$$\mu \frac{\partial^2 u}{\partial y^2} - \eta \frac{\partial^4 u}{\partial y^4} - \sigma B_0^2 u = \frac{\partial p}{\partial x} + \sigma E_z B_0 \qquad (1)$$

$$\frac{\partial p}{\partial y} = 0 \tag{2}$$

$$\frac{\partial u}{\partial x} + \frac{\partial v}{\partial y} = 0 \tag{3}$$

$$\int_{y=0}^{h} \left(E_z + B_0 u\right) dy = 0 \tag{4}$$

For the wide composite slider bearing, the film thickness can be written as

$$h = h_s + h_2 \tag{5}$$

$$h_s = \begin{cases} d\left\{1 - \left(x/L_1\right)\right\} & 0 \le x \le L_1 \\ 0 & L_1 \le x \le L \end{cases}$$

where d is the difference of inlet-outlet thickness.

The relevant boundary conditions are

(i)At the upper surface $y = h$

$$u = 0,\ v = 0 \ \text{(no slip)};\ \frac{\partial^2 u}{\partial y^2} = 0 \ \text{(vanishing of couple stresses)} \tag{6}$$

(ii)At the lower surface $(y = 0)$:

$$u = U,\quad v = 0\ ;\qquad \frac{\partial^2 u}{\partial y^2} = 0 \ \text{(vanishing of couple stresses)} \tag{7}$$

3. Solution of the problem

The solution of the equation (1) with boundary conditions (6), (7) and the use of condition (4) is obtained in the form

$$u = -\frac{U}{2}\xi_1 - \frac{h_2^2 h}{2l\mu M_0^2}\frac{\partial p}{\partial x}\xi_2 \tag{8}$$

where

$$\xi_1 = \xi_{11} - \xi_{12},\ \xi_2 = \xi_{13} - \xi_{14} \qquad \text{for } 4M_0^2 l^2/h_2^2 < 1 \tag{9a}$$

$$\xi_1 = \xi_{21} - \xi_{22},\ \xi_2 = \xi_{23} - \xi_{24} \qquad \text{for } 4M_0^2 l^2/h_2^2 = 1 \tag{9b}$$

$$\xi_1 = \xi_{31} - \xi_{32},\ \xi_2 = \xi_{33} - \xi_{34} \qquad \text{for } 4M_0^2 l^2/h_2^2 > 1 \tag{9c}$$

$M_0 = B_0 h_2 (\sigma/\mu)^{1/2}$ and $\eta/\mu = l^2$

The associated relations in equations (9a), (9b) and (9c) are given in the Appendix-A.

The integration of continuity equation (3) over the film thickness and the use of expression (8) for u and the boundary conditions (6) and (7) gives the modified one dimensional Reynolds equation in the form

$$\frac{\partial}{\partial x}\left\{ f(h,l,M_0)\frac{\partial p}{\partial x}\right\} = 6U\frac{dh}{dx} \tag{10}$$

where

$$f(h,l,M_0) = \begin{cases} \dfrac{6h_2^2h^2}{\mu l M_0^2}\left\{ \dfrac{A^2 - B^2}{\dfrac{A^2}{B}\tanh\dfrac{Bh}{2l} - \dfrac{B^2}{A}\tanh\dfrac{Ah}{2l}} - \dfrac{2l}{h}\right\} & \text{for } 4M_0^2l^2/h_2^2 < 1 \\ \dfrac{6h_2^2h^2}{\mu l M_0^2}\left\{ \dfrac{2\left(Cosh\left(h/\sqrt{2}l\right)+1\right)}{3\sqrt{2}Sinh\left(h/\sqrt{2}l\right) - h/l} - \dfrac{2l}{h}\right\} & \text{for } 4M_0^2l^2/h_2^2 = 1 \\ \dfrac{6h_2^2h^2}{\mu l M_0^2}\left\{ \dfrac{M_0\left(CosB_1h + CoshA_1h\right)}{h_2\left(A_2SinB_1h + B_2SinhA_1h\right)} - \dfrac{2l}{h}\right\} & \text{for } 4M_0^2l^2/h_2^2 > 1 \end{cases} \tag{11}$$

$A_2 = \left(B_1 - A_1Cot\theta\right)\ B_2 = \left(A_1 + B_1Cot\theta\right)$

Using the non-dimensional quantities

$x^* = \frac{x}{L},\ P^* = \frac{ph_2^2}{\mu UL},\ l^* = \frac{2l}{h_2},\ H = \frac{h}{h_2},\ L_1^* = \frac{L_1}{L},\ L_2^* = \frac{L_2}{L}$ in equation (10), the

nondimensional modified MHD couple-stress Reynolds equation is obtained in the form

$$\frac{\partial}{\partial x^*}\left\{Hf^*(H,l^*,M_0)\frac{\partial P}{\partial x^*}\right\} = 6\delta\frac{d}{dx^*}\left\{1-\left(x^*/L_1^*\right)\right\} \tag{12}$$

Where

$$H = h_s^* + 1,$$

$$h_s^* = \begin{cases} \delta\left\{1-\left(x^*/L_1^*\right)\right\} & 0 \le x^* \le L_1^* \\ 0 & L_1^* \le x^* \le 1 \end{cases} \tag{13}$$

$$f^*(H,l^*,M_0) = \begin{cases} \frac{12H}{l^*M_0^2}\left\{\frac{(A^{*2}-B^{*2})}{\frac{A^{*2}}{B^*}\tanh\frac{B^*H}{l^*}-\frac{B^{*2}}{A^*}\tanh\frac{A^*H}{l^*}}-\frac{l^*}{H}\right\} & \text{for } M_0^2l^{*2}<1 \\ \frac{12H}{l^*M_0^2}\left\{\frac{1+Cosh\left(\sqrt{2}H/l^*\right)}{\left(3/\sqrt{2}\right)Sinh\left(\sqrt{2}H/l^*\right)-\left(H/l^*\right)}-\frac{l^*}{H}\right\} & \text{for } M_0^2l^{*2}=1 \\ \frac{12H}{l^*M_0^2}\left\{\frac{M_0\left(CosB_1^*H+CoshA_1^*H\right)}{A_2^*SinB_1^*H+B_2^*SinhA_1^*H}-\frac{l^*}{H}\right\} & \text{for } M_0^2l^{*2}>1 \end{cases} \tag{14}$$

$$A^* = \left\{\frac{1+\left(1-l^{*2}M_0^2\right)^{1/2}}{2}\right\}^{1/2} \qquad B^* = \left\{\frac{1-\left(1-l^{*2}M_0^2\right)^{1/2}}{2}\right\}^{1/2}$$

$$A_1^* = \sqrt{2M_0/l^*}\,Cos\left(\theta^*/2\right)\ \ B_1^* = \sqrt{2M_0/l^*}\,Sin\left(\theta^*/2\right)\ \theta^* = \tan^{-1}\left(\sqrt{l^{*2}M_0^2-1}\right)$$

$$A_2^* = \left(B_1^* - A_1^*Cot\theta^*\right)\ B_2^* = \left(A_1^* + B_1^*Cot\theta^*\right)$$

Twice integration equation (10) with respect to x^* and the use of ambient boundary conditions $P^* = 0$ at $x^* = 0,\ 1$ gives

$$P_1^* = 6\int_{x^*=0}^{x^*} \frac{\delta\left(1 - x^*/L_1^*\right)}{Hf^*(H, l^*, M_0)}dx^* + C\int_{x^*=0}^{x^*} \frac{1}{Hf^*(H, l^*, M_0)}dx^* \quad 0 \le x^* \le L_1^* \tag{15a}$$

$$P_2^* = \frac{C\left(x^* - 1\right)}{f^*(1, l^*, M_0)} \quad L_1^* \le x^* \le 1 \tag{15b}$$

where

$$C = -\frac{6\int_{x^*=0}^{L_1^*} \frac{\delta\left(1 - x^*/L_1^*\right)}{Hf^*(H, l^*, M_0)}dx^*}{\left\{\int_{x^*=0}^{L_1^*} \frac{1}{Hf^*(H, l^*, M_0)}dx^* - \int_{x^*=1}^{L_1^*} \frac{1}{f^*(1, l^*, M_0)}dx^*\right\}} \tag{16}$$

The load per unit width is given by

$$w = \int_0^L p dx \tag{17}$$

The dimensionless load carrying capacity W^* is

$$W^* = \frac{wh_2^2}{\mu UL^2} = \int_{x^*=0}^{L_1^*} P_1^* dx^* + \int_{x^*=L_1^*}^{1} P_2^* dx^* \tag{18}$$

Using (15a) and (15b) the non dimensional load carrying capacity is obtained in the form

$$W^* = 6\int_{x^*=0}^{L_1^*}\int_{x^*=0}^{x^*} \frac{\delta(1 - x^*/L_1^*) + C}{f^*(H, l^*, M_0)}dx^* dx^* - \frac{C\left(1 - L_1^*\right)^2}{2f^*(1, l^*, M_0)} \tag{19}$$

The frictional force on the bearing surface is

$$F = \int_0^L \left(\tau_{21}\right)_{y=0} dx = \int_0^L \left\{-G(h, l, M_0) - \frac{h}{2}\frac{\partial p}{\partial x}\right\}dx \tag{20}$$

where

$$G(h,l,M_0)=\begin{cases}\dfrac{\mu U l M_0^2}{2h_2^2(A^2-B^2)}\left\{\dfrac{A^2}{B}\coth\left(\dfrac{Bh}{2l}\right)-\dfrac{B^2}{A}\coth\left(\dfrac{Ah}{2l}\right)\right\} & \text{for } M_0^2l^{*2}<1\\ \dfrac{\mu U}{16l^2}\left\{\dfrac{h+3\sqrt{2}lSinh\left(h/\sqrt{2}l\right)}{Cosh\left(h/\sqrt{2}l\right)-1}\right\} & \text{for } M_0^2l^{*2}=1\\ \dfrac{\mu U}{2}\left\{\dfrac{\left(K_1-K_2Cot\theta\right)SinhA_1h+\left(K_1Cot\theta+K_2\right)SinB_1h}{CoshA_1h-CosB_1h}\right\} & \text{for } M_0^2l^{*2}>1\end{cases} \quad (21)$$

$$K_1=\sqrt{M_0/lh_0}Cos\left(\theta/2\right)\left[1-\left(lM_0/h_0\right)\left\{1-4Sin^2\left(\theta/2\right)\right\}\right]$$

$$K_2=\sqrt{M_0/lh_0}Sin\left(\theta/2\right)\left[1+\left(lM_0/h_0\right)\left\{1-4Cos^2\left(\theta/2\right)\right\}\right]$$

The non dimensional frictional force is

$$F^*=-\frac{Fh_2}{6\mu UL}=\int_0^1\left\{G(H,l^*,M_0)+\frac{H}{2}\frac{\partial P^*}{\partial x^*}\right\}dx^* \quad (22)$$

Where

$$G^*(H,l^*,M_0)=\begin{cases}\dfrac{l^*M_0^2}{4(A^{*2}-B^{*2})}\left\{\dfrac{A^{*2}}{B^*}\coth\left(\dfrac{B^*H}{l^*}\right)-\dfrac{B^{*2}}{A^*}\coth\left(\dfrac{A^*H}{l^*}\right)\right\} & \text{for } M_0^2l^{*2}<1\\ \dfrac{1}{8l^{*2}}\left\{\dfrac{2H+3\sqrt{2}l^*Sinh\left(\sqrt{2}H/l^*\right)}{Cosh\left(\sqrt{2}H/l^*\right)-1}\right\} & \text{for } M_0^2l^{*2}=1\\ \dfrac{\left(K_1^*-K_2^*Cot\theta^*\right)SinhA_1^*H+\left(K_1^*Cot\theta^*+K_2^*\right)SinB_1^*H}{2\left(CoshA_1^*H-CosB_1^*H\right)} & \text{for } M_0^2l^{*2}>1\end{cases} \quad (23)$$

$$K_1^*=\sqrt{2M_0/l^*}Cos\left(\theta^*/2\right)\left[1-\left(l^*M_0/2\right)\left\{1-4Sin^2\left(\theta^*/2\right)\right\}\right]$$

$$K_2^*=\sqrt{2M_0/l^*}Sin\left(\theta^*/2\right)\left[1+\left(l^*M_0/2\right)\left\{1-4Cos^2\left(\theta^*/2\right)\right\}\right]$$

Using (15a) and (15b) in equation (22) the non dimensional frictional force is obtained in the form

$$F^*=-\frac{Fh_2}{\mu UL}=\left\{G^*(1,l^*,M_0)-\frac{3C_1}{f^*(1,l^*,M_0)}\right\}\left(1-L_1^*\right)+\int_0^{L_1^*}\left\{G^*(H,l^*,M_0)+\frac{3\delta\left(1-x^*/L_1^*\right)-3C_1}{f^*(H,l^*,M_0)}\right\}dx^* \quad (24)$$

The co-efficient of friction is given by

$$C = \frac{F^*}{W^*} \tag{25}$$

4. Results and discussion

The effect of couple stress and magnetic field is observed through the couple stress parameter l^* and the Hartmann number M_0 respectively. The parameter l^* is the ratio of microstructure size to the radial clearance.

4.1 Pressure

Figure 2 shows the variation of non dimensional film pressure with x^* for different values of Hartmann number M_0 and couple stress parameter l^*. It is observed that the non dimensional pressure p^* increases with increasing value of M_0 and l^*. The curves corresponding to $M_0=0$ and $l^*=0$ represents respectively the non-magnetic case and the Newtonian case. Figure 3 shows the variation of non dimensional maximum pressure $p^*_{\max}$ with L_1^* It is observed that, the non dimensional maximum pressure increases with L_1^* until a maximum is obtained, and there after decreases with L_1^*.

4.2 Load carrying capacity

Figure 4 shows the variation of non dimensional load carrying capacity with shoulder parameter δ for different values of M_0 and l^*. It is observed that the non dimensional load carrying capacity increases with increasing value of M_0 and l^* as compared to non magnetic case $M_0 = 0$ and Newtonian case $l^* = 0$. Figure 5 depict the variation of non dimensional maximum load carrying capacity with L_1^* for different values of M_0 and l^*. It is observed that the non-dimensional maximum load increases with L_1^* until a maximum is obtained, and there after decreases with L_1^*.

4.3 Frictional Force

Figure 6 depicts the variation of non dimensional frictional force F^* with shoulder parameter δ for different values of M_0 and l^*. It is observed that the non dimensional frictional force increases with increasing value of M_0 and l^* as compared to non magnetic case and Newtonian case. Figure 7 depicts the variation of non dimensional frictional force F^* with L_1^* for different values of M_0 and l^*. It is observed that the non-dimensional frictional force decreases with $L_1{}^*$ for Newtonian case, further increases with $L_1{}^*$ until a maximum is attained, and there after decreases with $L_1{}^*$ for non Newtonian case.

4.4 Co-efficient of Friction

Figure 8 shows the variation of non dimensional co-efficient of friction with shoulder parameter δ for different values of M_0 and l^*. It is observed that the non dimensional co-efficient of friction increases with the increasing value of M_0. Further, non dimensional co-efficient of friction decreases with increasing value of l^*. Figure 9 depicts the variation of non dimensional co-efficient of friction with $L_1{}^*$. It is observed that the non dimensional co-efficient of friction decreases with increasing value of $L_1{}^*$.

The relative percentage increase in the non-dimensional load carrying capacity $R_W{}^*$, non-dimensional frictional force $R_F{}^*$ and coefficient of friction R_C are defined by

$$R_{W^*} = \left\{\left(W^*_{magnetic} - W^*_{non-magnetic}\right)\Big/ W^*_{non-magnetic}\right\}\times 100$$

$$R_{F^*} = \left\{\left(F^*_{magnetic} - F^*_{non-magnetic}\right)\Big/ F^*_{non-magnetic}\right\}\times 100$$

and $$R_C = \left\{\left(C_{magnetic} - C_{non-magnetic}\right)\Big/ C_{non-magnetic}\right\}\times 100$$

The values of $R_W{}^*$, $R_F{}^*$ and R_C are listed in Table 1 for various values of l^*, M_0 with $L_1{}^* = 0.6$,

δ = 1.5. It is clear that an increase of nearly 132.63%, 348.61% and 92.84% in W^*, F^* and C is observed for l^* = 0.6 and M_0 = 6.

Numerical Example

For the industrial application the following numerical example of the MHD effect on wide composite slider bearing lubricated with couple-stress fluids is illustrated in table 2. Stokes [11] gives experimental measurements for the material constant η characterizing the couple-stress fluid which accounts for industrial oils with additives.

Conclusions

An analysis of the combined effects of MHD and couple stresses on the wide composite slider bearing is presented in this paper. It is found that the effect of couple stress is to increase the non dimensional pressure, load carrying capacity and frictional force but decrease the co-efficient of friction. The effect of magnetic field is to increase the non dimensional pressure, load carrying capacity, frictional and the co-efficient of friction.

Nomenclature

B_0 applied magnetic field

C coefficient of friction

d inlet-outlet thickness difference (h_1 - h_2)

F frictional force

F^* non-dimensional frictional force $\left(= -Fh_2 / \mu UL\right)$

h film thickness

h_1 inlet film thickness

h_1^* non-dimensional inlet film thickness

h_2 outlet film thickness

H non-dimensional film thickness $(= h/h_2)$

l couple stress parameter $(\eta/\mu)^{1/2}$

l^* non-dimensional couple stress parameter $(2l/h_2)$

L Bearing length

M_0 Hartmann number $(= B_0 h_2 (\sigma/\mu)^{1/2})$

p pressure in the film region

P^* non-dimensional pressure $(= ph_2^2/\mu UL)$

x, y rectangular coordinates

x^* non-dimensional rectangular coordinates $(x^* = x/L)$

u, v velocity components in film region

w load carrying capacity

W^* non-dimensional load carrying capacity $(= -wh_2^2/\mu UL^2)$

δ non-dimensional inlet-outlet thickness difference (d/h_2)

η material constant characterizing couple stress

μ viscosity coefficient

σ electrical conductivity

Appendix A

$$\xi_{11} = \frac{B^2}{(A^2 - B^2)}\left\{\frac{Sinh(Ah/l) - Sinh(Ay/l) - Sinh\, A(h-y)/l}{Sinh(Ah/l)}\right\} \quad \text{(A1a)}$$

$$\xi_{12} = \frac{A^2}{(A^2 - B^2)}\left\{\frac{Sinh(Bh/l) - Sinh(By/l) - Sinh\, B(h-y)/l}{Sinh(Bh/l)}\right\} \quad \text{(A1b)}$$

$$\xi_{13} = \frac{B^2\left\{Sinh(Ah/l) - Sinh(Ay/l) + Sinh\, A(h-y)/l\right\}}{Sinh(Ah/l)\left\{(B^2/A)\tanh(Ah/2l) - (A^2/B)\tanh(Bh/2l)\right\}} \quad \text{(A1c)}$$

$$\xi_{14} = \frac{A^2\left\{Sinh\left(Bh/l\right) - Sinh\left(By/l\right) + Sinh\,B(h-y)/l\right\}}{Sinh\left(Bh/l\right)\left\{\left(B^2/A\right)\tanh\left(Ah/2l\right) - \left(A^2/B\right)\tanh\left(Bh/2l\right)\right\}} \quad \text{(A1d)}$$

$$A = \left[\frac{1+\left\{1-\left(4l^2M_0^2/h_2^2\right)\right\}^{1/2}}{2}\right]^{1/2} \quad \text{(A1e)}$$

$$B = \left[\frac{1-\left\{1-\left(4l^2M_0^2/h_2^2\right)\right\}^{1/2}}{2}\right]^{1/2} \quad \text{(A1f)}$$

$$\xi_{21} = \frac{Sinh\left\{(y-h)/\sqrt{2}l\right\} + Sinh\left(y/\sqrt{2}l\right) - Sinh\left(h/\sqrt{2}l\right)}{Sinh\left(h/\sqrt{2}l\right)} \quad \text{(A2a)}$$

$$\xi_{22} = \frac{yCosh\left\{(y-h)/\sqrt{2}l\right\} + yCosh\left(y/\sqrt{2}l\right) - hCosh\left(h/\sqrt{2}l\right) - h}{2\sqrt{2}lSinh\left(h/\sqrt{2}l\right)} \quad \text{(A2b)}$$

$$\xi_{23} = \frac{ySinh\left\{(y-h)/\sqrt{2}l\right\} + ySinh\left(y/\sqrt{2}l\right) - hSinh\left(y/\sqrt{2}l\right)}{6lSinh\left(h/\sqrt{2}l\right) - \sqrt{2}h} \quad \text{(A2c)}$$

$$\xi_{24} = \frac{2Cosh\left\{(y-h)/\sqrt{2}l\right\} + 2Cosh\left(y/\sqrt{2}l\right) - 2Cosh\left(h/\sqrt{2}l\right) - 2}{3\sqrt{2}Sinh\left(h/\sqrt{2}l\right) - \left(h/l\right)} \quad \text{(A2d)}$$

$$\xi_{31} = \frac{CoshA_1\,yCosB_1\left(y-h\right) - CosB_1\,yCoshA_1\left(y-h\right)}{\left(CoshA_1h - CosB_1h\right)} \quad \text{(A3a)}$$

$$\xi_{32} = \frac{Cot\theta\left\{SinhA_1\,ySinB_1\left(y-h\right) - SinB_1\,ySinhA_1\left(y-h\right)\right\} + \left(CoshA_1h - CosB_1h\right)}{\left(CoshA_1h - CosB_1h\right)} \quad \text{(A3b)}$$

$$\xi_{33} = \frac{Cot\theta\left\{SinB_1\,ySinhA_1\left(y-h\right) + SinhA_1\,ySinB_1\left(y-h\right)\right\} + \left(CosB_1h + CoshA_1h\right)}{\left(B_1 - A_1Cot\theta\right)SinB_1h + \left(A_1 + B_1Cot\theta\right)SinhA_1h} \quad \text{(A3c)}$$

$$\xi_{34} = \frac{CosB_1\,yCoshA_1\left(y-h\right) + CoshA_1\,yCosB_1\left(y-h\right)}{\left(B_1 - A_1Cot\theta\right)SinB_1h + \left(A_1 + B_1Cot\theta\right)SinhA_1h} \quad \text{(A3d)}$$

$$A_1 = \sqrt{M_0/lh_0}\,Cos(\theta/2) \qquad \text{(A3e)}$$

$$B_1 = \sqrt{M_0/lh_0}\,Sin(\theta/2) \qquad \text{(A3f)}$$

$$\theta = \tan^{-1}\left(\sqrt{4l^2M_0^2/h_0^2 - 1}\right) \qquad \text{(A3g)}$$

References

[1] Ramanaiah G., and **Sarker P.,** Slider bearings lubricated by fluids with couple stress, Wear, 52, 1979, 27-36.

[2] Lin J. R., Lu R. F., and **Chang T. B.,** Derivation of dynamic couple-stress Reynolds equation of sliding squeezing surfaces and Numerical solution of plane inclined slider bearings, Tribol. Int., 36, 2003, 679-685.

[3] Bujurke N. M., Patil H.P., and **Bhavi S. G.,** Porous slider bearing with couple stress fluid, Acta Mechanica, 85, 1990, 99-113.

[4] Lin J. R., and Yu-Ming Lu., Steady-state performance of wide parabolic-shaped slider bearings with a couple stress fluid, J. of Marine Sci. and Tech.,12, 2004, 239-246.

[5] Naduvinamani N. B. and **Siddanagouda A**., A note on porous Rayleigh step bearings lubricated with couple stress fluids, JET, Vol. 221 Part J, 2007, 615-621.

[6] Lin J. R., Lu R. F. and **Hung C. R.,** Dynamic characteristics of wide exponential film-shape slider bearings lubricated with a non-Newtonian couple stress fluid, J. of Marine Sci. and Tech., Vol. 14, No. 2, 2006, 93-101,

[7] Lin J.R., Effect of couple stresses on the lubrication of finite journal bearings. Wear, 206, 1997, 171-178.

[8] Lin J. R., Lu R. F., Ho M. H. and **Lin M. C.,** Dynamic characteristics of wide tapered-land slider bearings, J. of Chinese Inst. of Engineers, Vol. 29, No. 3, 2006, 543-548.

[9] Ramanaiah G., Squeeze films between finite plates lubricated by fluids with couple stress, Wear, 54, 1979, 315-320.

[10] Bujurke N. M., and **Jayaraman G**., The influence of couple stresses in squeeze films, Int. J. Mech. Sci., 24, 1982, 369-376.

[11] Stokes K.V. Couple stresses in fluids, Physics of fluids, **9**, 1966, 1709-1715.

[12] Shukla J.B., The Magnetohydrodynamic composite slider bearing, Wear, 7, 1964, 460-465.

[13] Lin J. R., MHD steady and dynamic characteristics of wide tapered-land slider bearings, Tribology International, 43, 2010, 2378-2383.

[14] Naduvinamani N .B. **Fathima S.T**., and **Hanumagowda B. N**. Magnetoydrodynamic couplestress squeeze film lubrication of Circular Stepped Plates. JET, 225(3) Part J, 2011, 111-119.

[15] Malik M. and **Singh D. V**., Analysis of finite Magnetohydrodynamic journal bearings, Wear, 64, 1980, 271-280.

[16] Gupta J. L., and **Bhat M. V**., An inclined porous slider bearing with a transverse magnetic field, Wear, 55, 1979, 359-367.

[17] Rodkiewicz C. M. and **Anwar M. I.,** Effects of step type magnetic field in slider bearing, Wear, 21, 1972, 223-229.

[18] Snyder W. T., The magneto hydrodynamic slider bearing, J. Basic Engg., 85, 1963, 197-204.

[19] Shukla J.B., The optimum one-dimensional magneto-hydrodynamic slider bearing, ASME J. Lubr. Technol.,92, 1970, 530-534.

[20] Gupta R. S. and **Sharma L.G.,** Analysis of couple stress lubricant in hydrostatic thrust bearings. , Wear, 1988, 48, 257-269.

[21] Lin J. R., Hung C. R., Hsu C. H., and **Lai C**., Dynamic stiffness and damping characteristics of one-dimensional magneto-hydrodynamic inclined-plane slider bearings, JET, 223 Part J, 2009, 211-219.

[22] Hughes, W. F., The magneto hydrodynamic finite step slider bearing, Journal of Basic Engineering, Vol. 85, 1963, 129-136.

[23] Kamiyama, S., Magnetohydrodynamic journal bearing (Report 1), Journal of Lubrication Technology, Vol. 91, 1969, 380-386 .

[24] Kuzma, D. C., The magnetohydrodynamic journal bearing, Journal of Basic Engineering, Vol. 85, 1963, 424-428.

[25] Lin, J. R., Magnetohydrodynamic lubrication of finite slider bearings, International Journal of Applied Mechanics and Engineering, Vol. 7, 2002, 1229-1246.

[26] Lin J. R., and **Lu R. F**., Dynamic characteristics for Magneto-hydrodynamic wide slider bearings with an exponential film profile, J. of Marine sci. and Tech., Vol. 18, No 2, 2010, 268-276

[27] Hughes W. F., The Magnetohydrodynamic inclined slider bearings with a transverse magnetic field, Wear, 6, 1963, 315-324.

[28] Osterle J. F., and **Young F. J.,** On the load capacity of the hydro magnetically lubricated slider bearing, Wear, 5, 1967, 227-234.

[29] Tsu-Liang Chou, Jen-Wen Lai., and **Lin J. R.,** Magneto-hydrodynamic squeeze film characteristics between a sphere and a plane surface, J. of Marine Sci. and Tech., 11, 2003, 174-178.

[30] Lin J. R., Chou T. L., Chiang H. L. and **Chang C. Y.,** Non-Newtonian couple stress effects on the frictional and flow-rate performance of wide composite slider bearings, Nanya.edu.tw, 2010, 35-46.

Acknowledgement

The corresponding author sincerely thanks to financial assistance by U.G.C. New Delhi, India. Vide order number F. 41-775/2012(SR) under major project.

Figures

Figure 1 Wide composite slider Bearing.

Figure 2 Variation of non dimensional pressure P^* with x^* for different values of M_0 and l^* with $L_1^* = 0.6$, $\delta^* = 1.5$.

Figure 3 Variation of non dimensional maximum pressure $P^*_{\max}$ with L_1^* for different values of M_0 and l^* with $\delta^* = 1.5$.

Figure 4 Variation of non dimensional load carrying capacity W^* with δ for different values of M_0 and l^* with $L_1^* = 0.6$.

Figure 5 Variation of non dimensional load carrying capacity W^* with L_1^* for different values of M_0 and l^* with $\delta = 1.5$.

Figure 6 Variation of non dimensional frictional force F^* with δ for different values of M_0 and l^* with $L_1^* = 0.6$.

Figure 7 Variation of non dimensional frictional force F^* with L_1^* for different values of M_0 and l^* with $\delta = 1.5$.

Figure 8 Variation of co efficient of friction C with δ for different values of M_0 and l^* with $L_1^* = 0.6$.

Figure 9 Variation of co efficient of friction C with L_1^* for different values of M_0 and l^* with $\delta = 1.5$.

Tables

Table1 Variation of R_W^*, R_F^* and R_C for different values l^* and M_0 with $L_1^* = 0.7$, $\delta = 1.5$.

Table 2 Numerical example of wide composite slider bearing with MHD and couple-stress fluid

Table 3 MHD and couple stress characteristics W^*, F^*, C and comparison with non magnetic case by Lin et al. [30] with $L_1^* = 0.7$, $l^* = 0.3$.

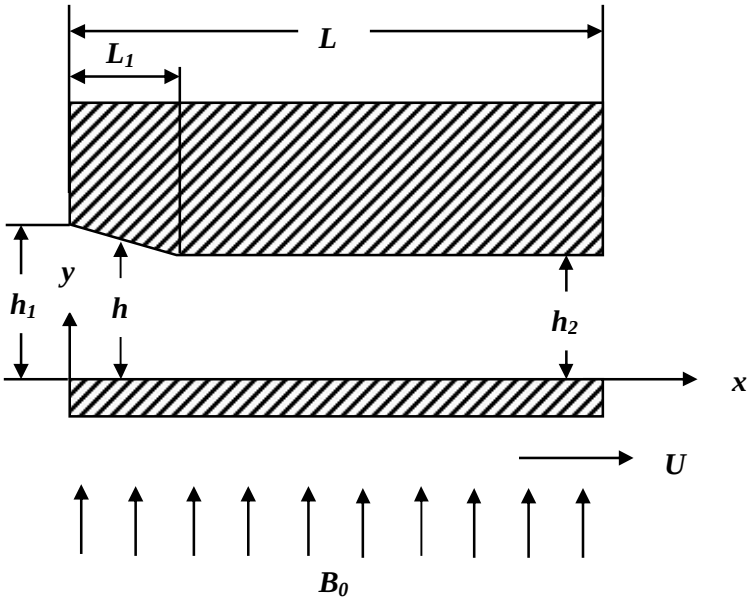

Figure 1 Wide composite slider Bearing.

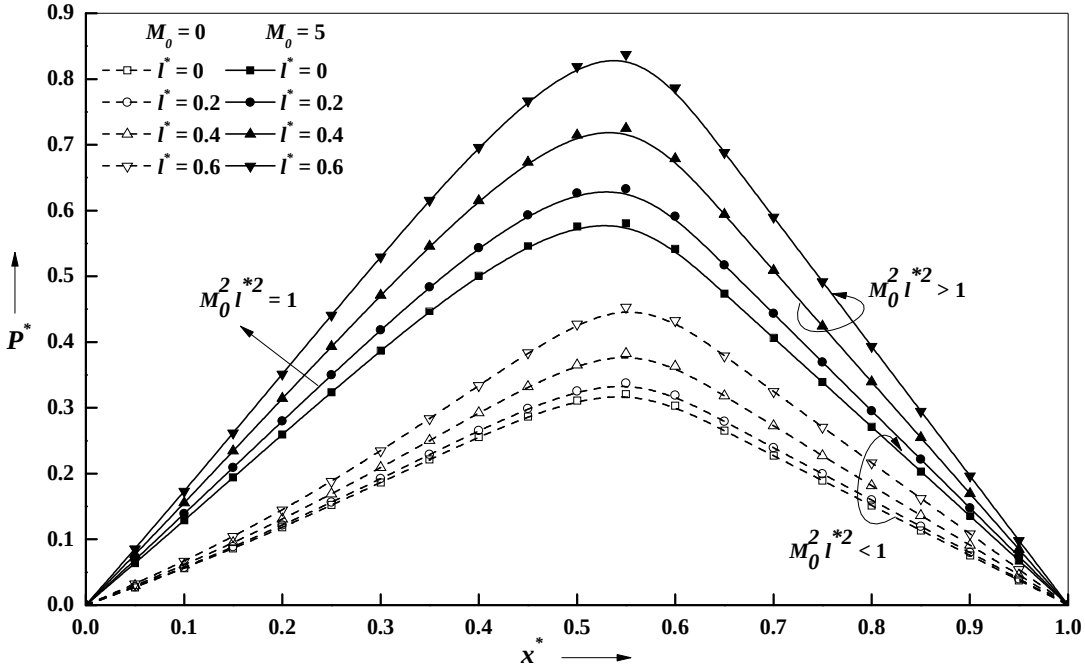

Figure 2 Variation of non-dimensional pressure P^* with x^* for different values of M_0 and l^* with $L_1^* = 0.6$, $\delta = 1.5$.

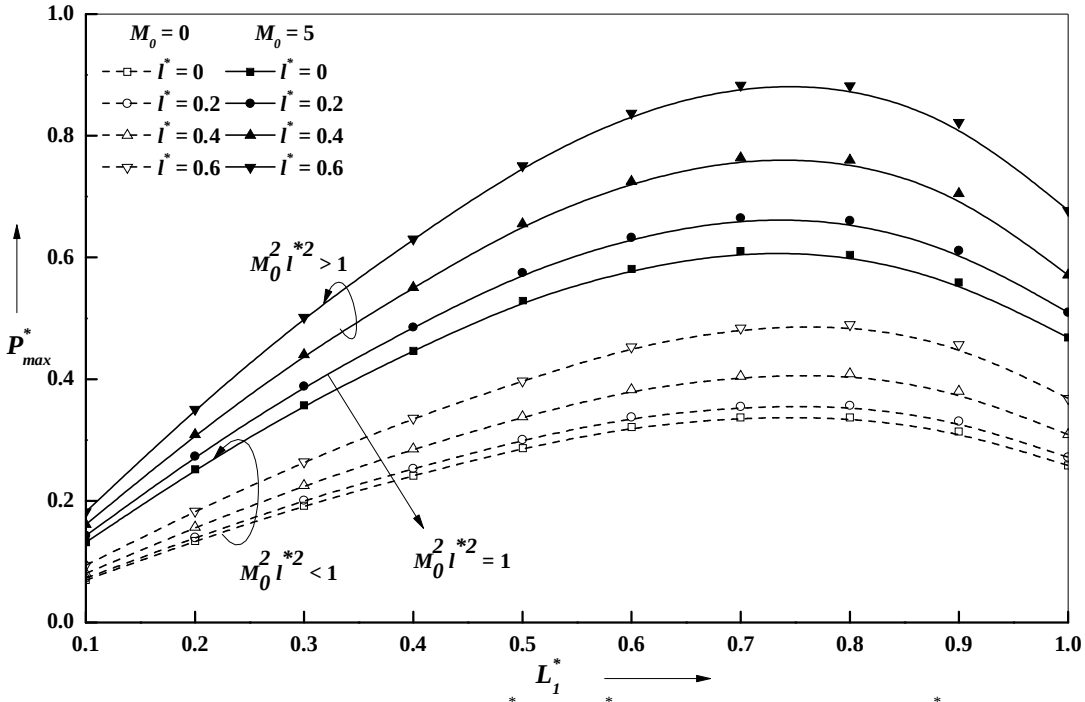

Figure 3 Variation of non-dimensional pressure P^*_{max} with L_1^* for different values of M_0 and l^* with $\delta = 1.5$.

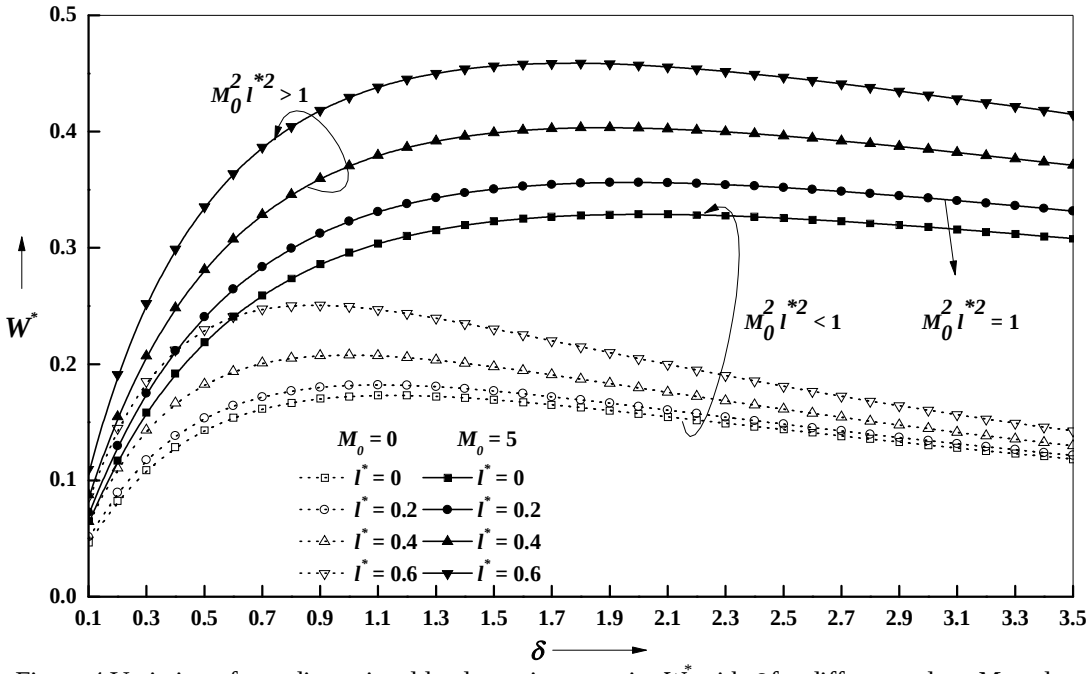

Figure 4 Variation of non dimensional load carrying capacity W^* with δ for different values M_0 and l^* with $L_1^* = 0.6$.

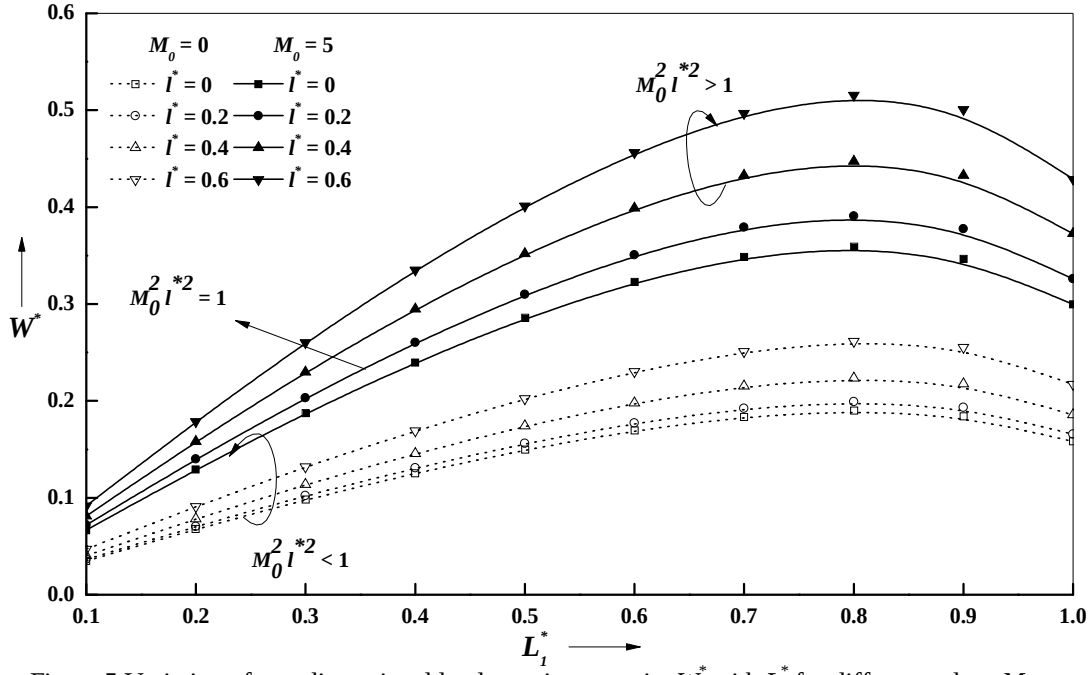

Figure 5 Variation of non dimensional load carrying capacity W^* with L_1^* for different values M_0 and l^* with $\delta = 1.5$

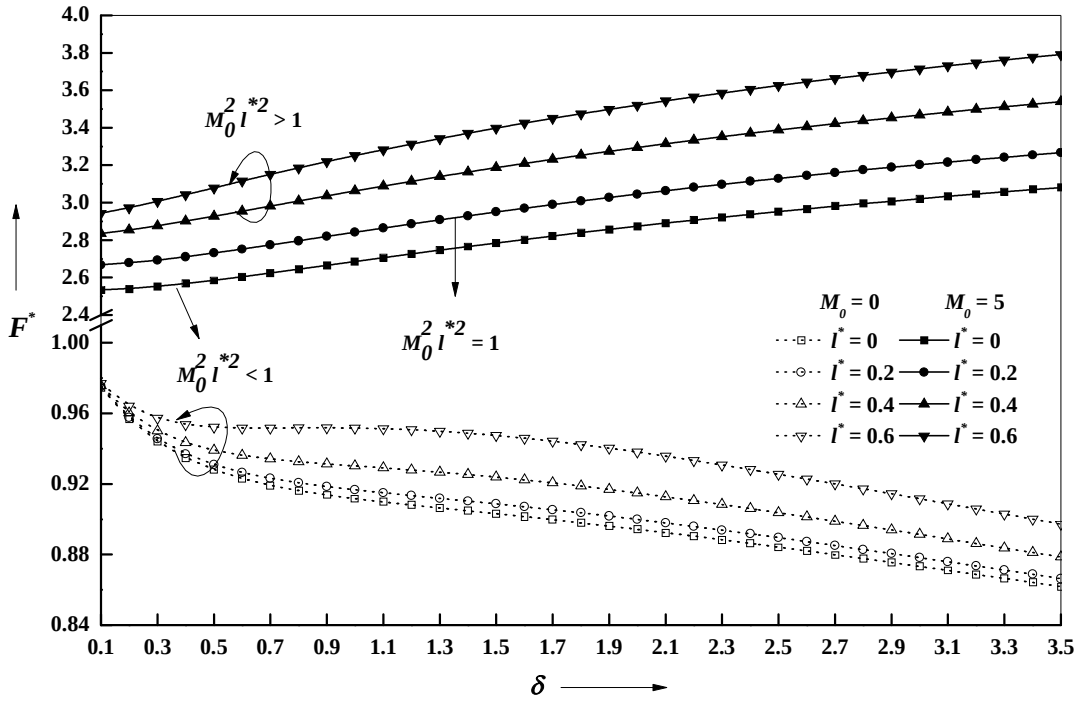

Figure 6 Variation of non dimensional frictional force F^* with δ for different values M_0 and l^* with $L_1^* = 0.6$.

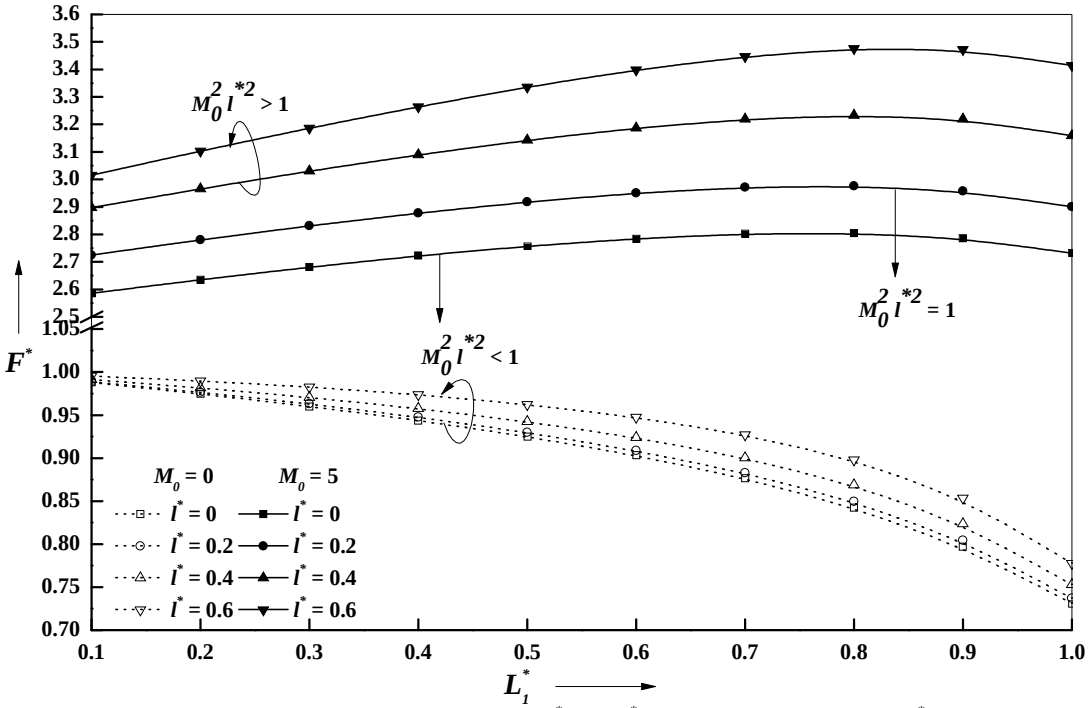

Figure 7 Variation of non dimensional frictional force F^* with L_1^* for different values M_0 and l^* with $\delta = 1.5$.

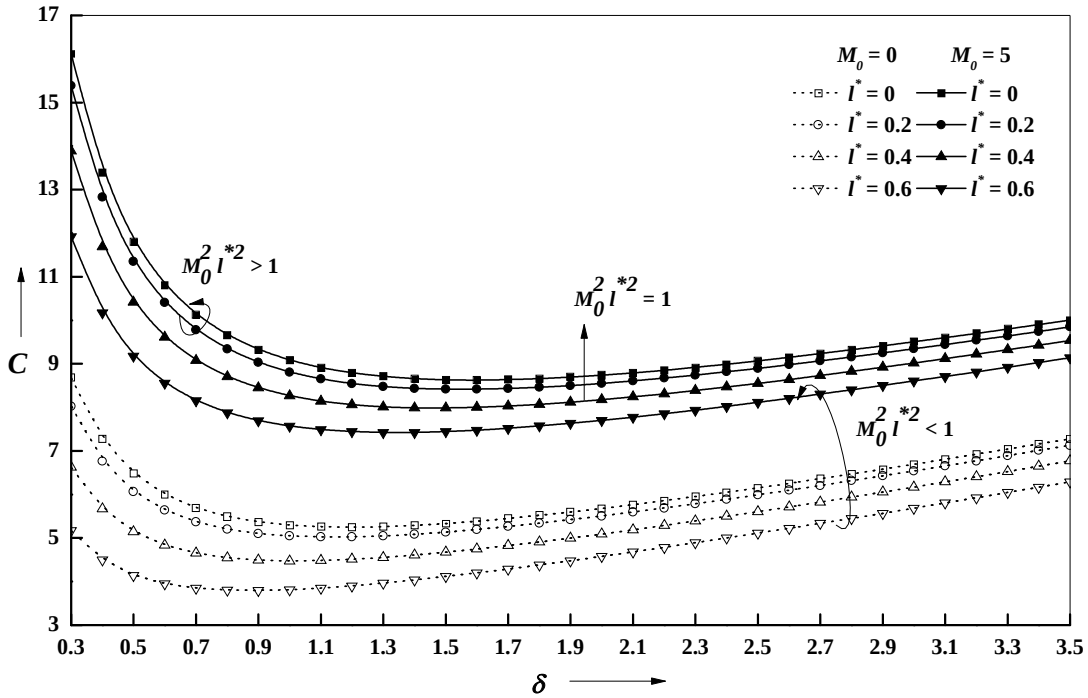

Figure 8 Variation of co efficient of friction C with δ for different values M_0 and l^* with $L_1^* = 0.6$.

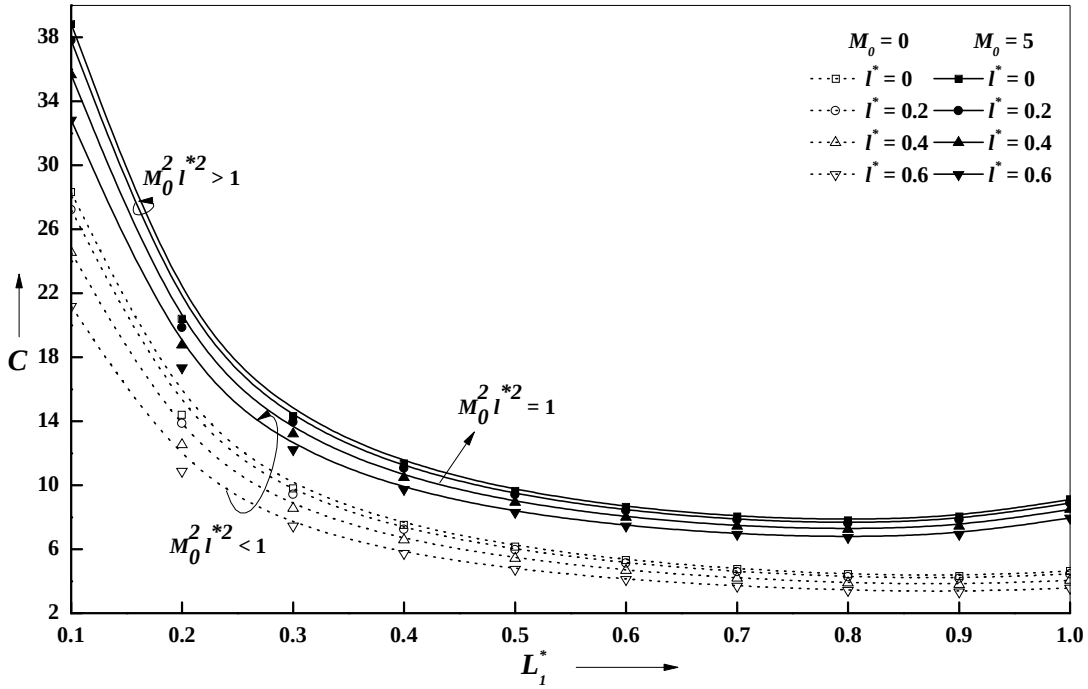

Figure 9 Variation of co efficient of friction C with L_1^* for different values M_0 and l^* with $\delta = 1.5$.

Table1 Variation of R_W^*, R_F^* and R_C for different values l^* and M_0 with $L_1^* = 0.6$, $\delta = 1.5$.

l^*	M_0	R_W^*	R_F^*	R_C
0	3	41.1280	97.108	39.666
	6	117.031	266.938	69.072
	9	199.470	445.435	82.133
0.3	3	43.2720	103.043	41.718
	6	134.158	310.523	75.319
	9	246.104	559.452	90.536
0.6	3	40.2020	107.408	47.936
	6	132.625	348.606	92.844
	9	250.811	659.618	116.532
0.9	3	33.5370	107.089	55.079
	6	116.270	364.312	61.834
	9	225.347	710.871	87.872

Table 2 Numerical example of wide composite slider bearing with MHD and couple-stress fluid

Physical parameter	Notation	Range of values chosen
Length of the bearing	L	1.00×10^{-1} m
Length of the inclined part	L_1	$(0.1,0.2,0.3,0.4,0.5,0.6,0.7,0.8,0.9,1.0) \times 10^{-1}$m
Minimum film thickness	h_2	0.5×10^{-4} m
Inlet-outlet thickness difference	h_1- h_2	$(0.05$ to $0.175) \times 10^{-4}$ m
Electrical conductivity	σ	$1.07 \times 10^{6} mh_0 / m$
Applied magnetic field	B_0	$0,1.52,3.04,4.56 Wb/m^2$
Lubricant viscosity	μ	$1.55 \times 10^{-3} Pa.s$
Couple stress material constant	η	$0,0.3875,1.55,6.2 \times 10^{-13}$N.s

Table 3 MHD and couple stress characteristics W^*, F^*, C and comparison with non magnetic case (NMC) by Lin et al. [30] with $L_1^* = 0.6$, $l^* = 0.3$.

	δ	NMC	Present Analysis			
			$M_0 = 0$	$M_0 = 3$	$M_0 = 6$	$M_0 = 9$
W^*	0.5	0.166265	0.165845	0.202193	0.294572	0.419622
	1.0	0.193198	0.192877	0.25534	0.398195	0.580163
	1.5	0.186036	0.185804	0.266206	0.435075	0.643075
	2.0	0.170541	0.170374	0.262525	0.44384	0.662862
	2.5	0.154051	0.153931	0.253465	0.439688	0.6619
F^*	0.5	0.934506	0.934399	1.71918	3.47782	5.62098
	1.0	0.92257	0.922422	1.78953	3.62021	5.8283
	1.5	0.915361	0.915209	1.85827	3.75714	6.03536
	2.0	0.906445	0.906304	1.91808	3.87917	6.22363
	2.5	0.895742	0.895616	1.96910	3.9859	6.39063
C	0.5	5.62057	5.63418	8.50267	11.8063	13.3953
	1.0	4.77527	4.78242	7.00841	9.09155	10.046
	1.5	4.92035	4.92566	6.98056	8.63563	9.38516
	2.0	5.31513	5.31949	7.30627	8.74002	9.38903
	2.5	5.81456	5.8183	7.76872	9.0653	9.65497